

Tilted orientation of molecular chains at the surface of a series of perfluoropolyether liquids: an X-ray photoelectron spectroscopic investigation

By V. BINDU, K. SMITHA and T. PRADEEP

Department of Chemistry and Regional Sophisticated Instrumentation Centre,
Indian Institute of Technology, Madras 600036, India

(Received 18 June 1997; accepted 14 July 1997)

Angle resolved X-ray photoelectron spectroscopic (XPS) studies of a series of perfluoropolyethers of general formula $F[\text{CF}(\text{CF}_3)\text{CF}_2\text{O}]_n\text{CF}_2\text{CF}_3$, where $n = 27, 65$, and >70 , show that there is preferential ordering of $-\text{CF}_3$ groups at the liquid surfaces. The C 1s intensity corresponding to the $-\text{CF}_3$ groups increases with decrease in the electron take-off angle. No measurable change in the oxygen or fluorine intensity is observed upon varying the electron take-off angle. However, experiments show that no adsorption site exists at the surfaces, indicating that the ether oxygens are not available for any of the surface processes. Relative enhancement of the C 1s intensity of the $-\text{CF}_2/\text{CF}_3$ group with decreasing take-off angle is different for different liquids, with smaller chain length liquids showing a more rapid change. This is explained as due to an increase in helicity and tilt of molecular chains from the surface normal. Computational studies have been performed at the semiempirical level to understand the molecular structure. XPS data along with the computational studies suggest that at the liquid–air interface the molecular chains are ordered nearly perpendicular to the surface with a tilt which increases with chain length. The conclusions are in agreement with recent atomic and molecular beam scattering, ion/surface scattering and theoretical modelling studies.

1. Introduction

In the recent past there have been intense efforts to understand interfacial phenomena. Of the interfaces, the vapour–liquid interface or the free liquid surface has received much attention. ‘Surface’ in a liquid refers to the region where drastic changes (10–90%) in macroscopic properties such as density, take place. This region in most liquids is of the order of 3–5 Å [1]. Properties of liquids such as dissolution, adhesion, lubrication and wetting depend largely on the atomic level structure at the surface. The equilibrium and non-equilibrium properties at the interfaces require an understanding of the molecular structure at the free liquid surface. Molecular dynamics and associated techniques [2–10] have contributed immensely to this. The experimental liquid surface structure is hard to investigate by conventional techniques due to changes in the instantaneous molecular configurations in the time scale of the experiment. Techniques such as light scattering [11], X-ray and neutron diffraction [12, 13] have contributed to the present understanding of liquids; however, information on molecular structure is hard to obtain.

Of late a number of other experimental techniques have been applied to improve our understanding of

the molecular level structure of liquids. Ion scattering techniques, both in low and high energy regimes, is highly surface sensitive [14]. Since the ion–surface interaction time is of the order of picoseconds [15], molecular motion of the liquid does not cause problems for the measurements. It may be mentioned that below a collision energy of 100 eV the ion beam samples only the first atomic layer. Moreover, experiments using self-assembled monolayers (SAMs) [15, 16] have shown that the technique is sensitive to the top functionality only. Due to these advantages, the technique is important for investigating dynamic systems such as liquids. In this context, it may be mentioned that a variation of the ion scattering technique, such as secondary ion mass spectrometry (SIMS) [17], in the low energy regime, referred to as chemical sputtering [18], could also serve very well for the objective mentioned. Recently one of us performed such a study on the surface of a perfluoropolyether liquid and concluded that the liquid surface shows a high degree of order with the CF_3 groups oriented nearly normal to the surface [19].

Just like ion scattering, atomic and molecular beam scattering experiments [20] also can reveal the true surface structure of liquids. By looking at the variation in the intensities of inelastic scattering and trapping

desorption peaks on a variety of surfaces, Nathanson and colleagues [20, 21] concluded that the surfaces of hydrocarbon liquids are composed of chain ends. The incident atoms undergo hard sphere-like collisions with the $-\text{CH}_2$ or $-\text{CH}_3$ groups protruding from the surface. Similar experiments have been performed on other liquids [22]. Yoon *et al.* [23] studied the structure and properties of thin films of binary mixtures of rod like and flexible polyimides using dielectric relaxation and X-ray photoelectron spectroscopy (XPS) and concluded that the surface properties of the mixture are dominated by the flexible molecule. Toney and Brennan [24] studied the X-ray reflectivity of thin layers of perfluoropolyether (PFPE) molecules with piperonyl end groups adsorbed on amorphous carbon thin films. Analyses of the mass density profile of the polymer layers suggest that the piperonyl end groups are preferentially adsorbed near the carbon film and the PFPE chains remain close to the surface. Specular reflection of X-rays has been used to study alkylsiloxane monolayers [25]. Information on the orientation of molecules which form the outermost layer of the liquid surface can be obtained from metastable impact electron spectroscopy (MIES) also. Using this, Keller *et al.* [26] studied liquid formamide and concluded that molecules of the topmost layer of the surface are oriented in such a way that their molecular plane is nearly parallel to the overall surface. Using infrared-visible sum-frequency generation, the molecular ordering at interfaces of common liquids can be inferred [27]. Polarization dependence and the phase of nonlinear susceptibility led Superfine *et al.* [28] to conclude that the methyl groups in methanol point away from the liquid surface.

The majority of the available information on liquid surface structure is from theoretical modelling. Using molecular dynamics modelling, Harris [2] suggests that the outer edge of n-alkanes, decane and ecosane liquids is dominated by chain ends. Matsumoto and Kataoka [29] investigated the properties of the liquid–vapour interface of methanol and water by computer simulations using molecular dynamics. Orientational structuring near the surface was studied also, and it was concluded that methanol projects its methyl group towards the vapour phase. For water, two types of orientation are found; in the vapour side one hydrogen atom is projected towards the vapour and in the liquid side the molecule prefers to lie down on the surface with both hydrogen atoms slightly directed to the liquid. Theoretical studies have been supported by surface potential measurements [30].

The more traditional method of surface science, namely photoelectron spectroscopy, however, has been applied very rarely to the study of liquids. The advantages such as the high surface sensitivity and fast time

scale of the process (10^{-16} s) can be used effectively in understanding dynamic systems such as liquids. The surface sensitivity of the technique could be varied by changing the electron take-off angle. The escape depth of electrons of about 1000 eV kinetic energy in organic materials is of the order of 30–60 Å [31]. This is comparable with the molecular dimensions of certain liquids. Therefore, a study of angle dependent photoemission intensity could be a direct way of measuring the variation in the chemical constitution as one approaches a liquid surface. Incidentally, this kind of investigation on liquids is not very easy, owing to the difficulties associated with maintaining a liquid in an ultra high vacuum. However, of late several liquids of extremely low vapour pressures have been available which made experimental investigations in an ultra high vacuum feasible.

In this paper, we discuss the results of a photoelectron spectroscopic investigation of the surface chemical composition of a variety of liquid perfluoropolyethers. Earlier work in this area has been the subject of two short papers which were concerned only with X-ray photoelectron spectroscopy [32, 33]. We include a summary of the earlier results also here for the sake of completeness. In addition to XPS, we have also used Auger electron spectroscopy (AES) for the purpose. Our studies performed on three different liquids of the same general chemical formula with different chain lengths show that the surface structure of chemically similar liquids is largely similar, although there are certain variations with regard to the extent of surface order. The study suggests that liquid chain ends are projected towards the surface, but tilted from the surface normal. The tilt angle increases with the chain length. These conclusions generally are in agreement with theoretical calculations and earlier experimental investigations. The results suggest that the chemical inertness, hydrophobicity and wetting properties of perfluoropolyethers are due to the presence of $-\text{CF}_3$ groups at the surface. Oxygen atom concentration does not vary to any detectable extent as the surface sensitivity of the measurement increases. However, adsorption measurements suggest that no adsorption site exists at the surface. It is important to note that both XPS and AES show preferential surface segregation of $-\text{CF}_3$ groups. We have estimated the region of preferential surface order in these liquids to be about 8 Å [34].

2. Experiment

Measurements were made using a VG Escalab Mk II spectrometer with non-monochromatic Mg K_{α} radiation at a base pressure of 8×10^{-10} Torr. The samples were prepared on 1000 Å thick gold coated polished glass substrates (with a 50 Å layer of Cr in between to increase

adhesion) by applying a 0.2 mm film of the liquid. To make the film, a few drops of the liquid were placed on the clean gold coated glass plate which was held in an inclined position. The liquid spreads on the surface as a neat film and the excess is drained. The thickness of the film formed at the surface is calculated from the mass of the liquid, its density and the area of the gold coated glass. The liquids used were three perfluoropolyethers [35] $F[CF(CF_3)CF_2O]_nCF_2CF_3$, where $n = 27, 65, >70$, with trade names krytox 1625, krytox 16256 and krytox 16350. The general properties of the liquids are shown in table 1. The sample manufactured by Dupont was a gift from Professor R. G. Cooks of Purdue University. The first sample, krytox 1625, showed some deterioration upon exposure to X-rays because of which there was a change in the spectrometer vacuum, whereas no change was observed for the other two samples. All the spectra are averages of 10 scans of 60 s duration. All the spectra were accumulated with 20 eV pass energy.

The electron take-off angle, defined as the angle between the photoelectron collection lens and the surface parallel, was varied by rotating the sample using the xyz manipulator of the instrument. At each take-off angle, a fresh layer of liquid was exposed to the X-ray flux. This was accomplished by allowing the excess liquid accumulated on one side of the substrate during an hour long measurement to flow to the opposite side. Photoelectron spectra at various take-off angles in the range $90^\circ - 10^\circ$ were measured. In all the cases, spectra at the same take-off angles could not be measured due to a change in the dimension of the glass plate restricting its rotation in the analysis chamber owing to the protruding X-ray gun and electrostatic lens. The glass plates used were of 1 cm^2 and 4 cm^2 area; larger glass plates were used for krytox 1625 and 16250. This was necessary to ensure that the area probed by the X-ray (3 mm^2) is of uniform thickness. In krytox 16350, due to its higher viscosity, the thickness does not vary substantially during a measurement. The XPS binding energies are referred to the Ag $3d_{5/2}$ peak at 368.2 eV. The binding energies presented here are not precise due to small changes in the

film thickness between measurements, and as a result the extent of charging varied. The variation in film thickness and concomitant changes in charging potential resulted in significant changes in the width of the peaks. In order to reduce the error, the acquisition time was kept low. A curve fitting program was applied to the C 1s data of the three samples.

Quantum chemical calculations were carried out with the Gaussian 94 system of programmes [36] using the complete neglect of differential overlap (CNDO) approximation [37]. The method is well documented [38, 39] and has been applied to a number of systems. The large size of the systems involved did not permit us to undertake *ab initio* molecular orbital (MO) calculations on them. Since our objective was limited to an understanding of the qualitative changes in the structure of the molecules with increase in chain length, a more exact calculation was not necessary.

3. Results and discussion

3.1. Molecular structure

Prior to a discussion of the experimental results, it is necessary to understand the structure of krytox molecules. Figure 1 shows the space filling structure of a lower member of the krytox series, $F[CF(CF_3)CF_2O]_nCF_2CF_3$. This structure has been fully optimized at the CNDO level of theory. The molecule assumes a helical structure. The extent of helicity increases with increase in polymer chain length. To understand this, we performed geometry optimizations

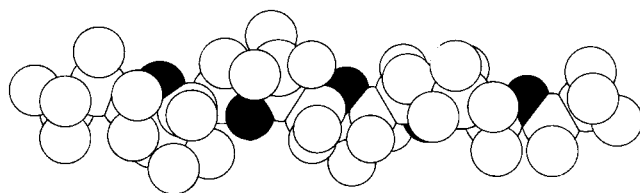


Figure 1. Space filling model of $F[CF(CF_3)CF_2O]_nCF_2CF_3$. The structure is fully optimized at the CNDO level of theory. The darker circles represent oxygen, larger circles represent carbon and the smaller circles represent fluorine.

Table 1. Some important properties of the krytox lubricants used in this investigation.

Trade name	Molecular weight	Vapour pressure Torr ^a	Viscosity centistokes ^a	Density g cm ⁻³ ^a
Krytox 1625	4600	3×10^{-10}	256	1.90
Krytox 16256	11 000	3×10^{-14}	2717	1.92
Krytox 16350	<15 000	$<4 \times 10^{-15}$	3500	<1.95

^aProperties listed are at 20 °C.

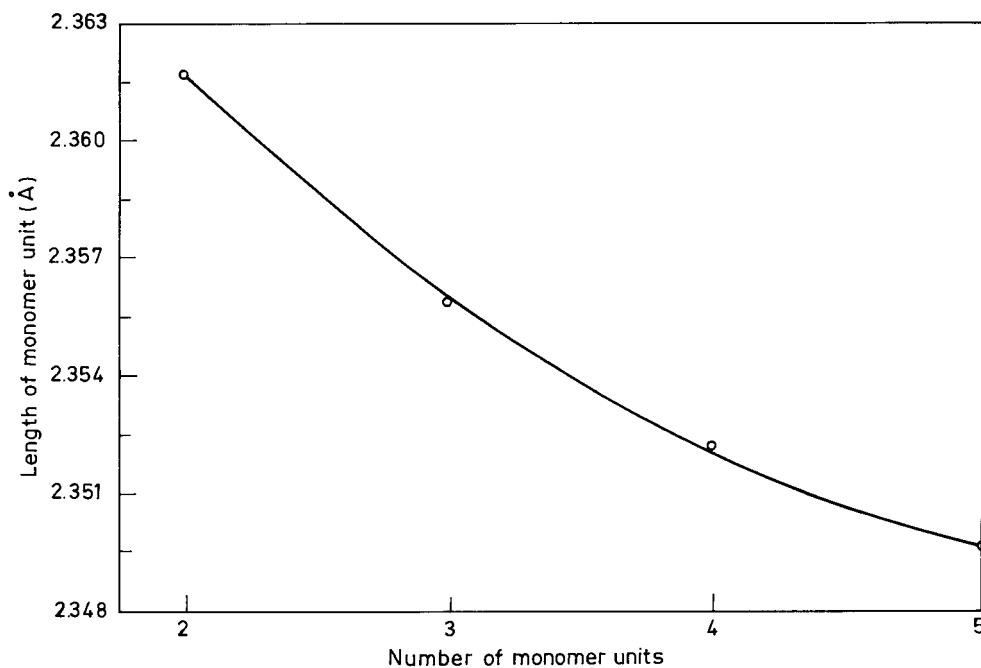


Figure 2. Plot of the variation of the monomer length with increasing number of repeating units (the extent of helicity also increases with chain length).

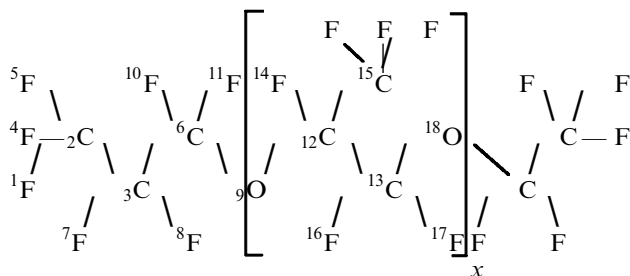
of molecules containing 2, 3, 4 and 5 repeating units. The optimized molecular parameters are given in table 2. An increase in helicity is manifested as an increase in the oxygen atom dihedral angles and a reduction in the carbon atom (other than the side chain) dihedral angles. As the number of monomer units increase from 2 to 5, the oxygen atom dihedral angles increase from 186.28°

to 187.59° with in-between values for the molecules containing 3 and 4 monomer units. This increase in dihedral angle results in a decrease in the length of the repeating unit as the chain length increases. In longer chains, higher helicity results in a more tightly packed structure. As a result, the molecule appears like a cylinder with fluorine atoms occupying the surface. Figure 2 shows the variation in monomer length with chain length. As one would expect, the variation is more pronounced between chains containing 2 and 3 units but tails off rapidly with increasing chain length.

Table 2. Important molecular parameters of krytox molecules obtained from molecular orbital calculations.^a

Parameters ^b	x = 1	x = 2	x = 3	x = 4
$r(\text{C}_2\text{C}_3)$	1.491	1.492	1.492	1.492
$r(\text{C}_6\text{O}_9)$	1.380	1.381	1.382	1.382
$a(\text{C}_2\text{C}_3\text{C}_6)$	112.34	112.46	112.57	112.67
$a(\text{C}_3\text{C}_6\text{O}_9)$	110.58	110.10	109.81	109.60
$a(\text{C}_6\text{O}_9\text{C}_{12})$	106.79	106.32	106.07	105.93
$d(\text{O}_9\text{C}_{12}\text{C}_{13}\text{O}_{18})$	186.28	187.16	187.41	187.59
$d(\text{C}_3\text{C}_6\text{O}_9\text{C}_{12})$	159.18	159.04	158.88	158.85
$d(\text{C}_6\text{O}_9\text{C}_{12}\text{C}_{13})$	169.63	169.47	169.30	169.23

^a The numbering scheme refers to the structure



^b r , distance; a , angle; and d , dihedral angle.

3.2. X-Ray photoelectron spectroscopy

3.2.1. General features

In all the three perfluoropolyether liquids there are four distinctly different carbon atoms, namely those associated with CF_3 groups, two different kinds of CF_2 group and CF groups. In a single molecule of each PFPE, the number of carbon atoms of different kinds are, krytox 1625: 28 CF_3 , 29 CF_2 and 26 CF , krytox 16256: 66 CF_3 , 67 CF_2 and 64 CF and krytox 16350: >71 CF_3 , >72 CF_2 and >69 CF . In each molecule, there are two CF_2 groups at the chain ends and the remaining CF_2 groups are in the repeating monomer unit. It is difficult to differentiate the two terminal CF_2 groups from the other CF_2 groups. The binding energies of CF_2 and CF_3 carbons will be close to each other since the CF_2 groups are attached to oxygen atoms in the repeating unit. It is hard to distinguish the two with a non-monochromatic X-ray source. However, CF carbon

will have a substantially lower binding energy. Therefore, the C 1s region of PFPE is expected to show two peaks corresponding to CF group and CF₂/CF₃ group ionizations, with the latter group having a higher binding energy. Since the cross-sections for the various carbon atoms are assumed to be the same, the intensity ratio of the peaks will be roughly 1:2 for the molecule and bulk liquid.

In addition to cross-sections, the actual intensities depend on electron take-off angle and the molecular ordering in the liquid. In the PFPE structure, the alternating CF₃ groups and the ether oxygens modify the tightly packed perfluoroalkane structure. It has been shown that the ether oxygens increase the flexibility [40]. If the molecules are not ordered, there will not be any change in the spectrum with angle regardless of whether surface or bulk is examined. If the molecules lie horizontal to the surface, the C 1s spectrum is expected to be the same with two components of roughly 1:2 intensity ratio at all angles. If the molecules are ordered laterally with the molecular axis nearly perpendicular to the surface, the C 1s intensities will vary significantly with the electron take-off angle. The intensity of the peak due to terminal CF₂ and CF₃ groups will increase with respect to CF groups as the electron take-off angle decreases.

At this point it is important to recall that the electron take-off angle will vary with the depth of the film that is sampled. When the photoelectron mean free path is 60 Å, the number of monomer units contributing to the PES intensity with a perpendicularly ordered structure is about 20. Then there are about 21 CF₃, 22 CF₂ and 19 CF groups per molecule contributing to the C 1s intensity. As the electron take-off angle decreases, the number of monomer units contributing to the PES intensity also decreases. As the depth sampled is decreased from 71.18 to 60.86 to 40.25 to 29.96 to 19.66 to 9.34 Å, the number ratio of CF₂/CF₃ to CF decreases from 43:19 to 31:14 to 25:11 to 19:8 to 13:5 to 7:2. Those numbers are calculated from the structure of a chain containing 20 repeating units. We have assumed the optimized molecular parameters of F[CF(CF₃)CF₂O]_nCF₂CF₃ to calculate these numbers.

3.2.2. XPS results

This change in intensity ratio is clearly visible in the photoelectron spectra of the three PFPE liquids (figures 3, 4, and 5), where the dots are original data points and the smooth lines are the results of the curve fitting procedure. In figure 3 the XPS spectra of C 1s region of krytox 1625 at various electron take-off angles are shown. The two bands at 292.3 eV and 294.3 eV correspond to CF and CF₂/CF₃ groups, respectively. As the electron take-off angle decreases, it can be seen that the

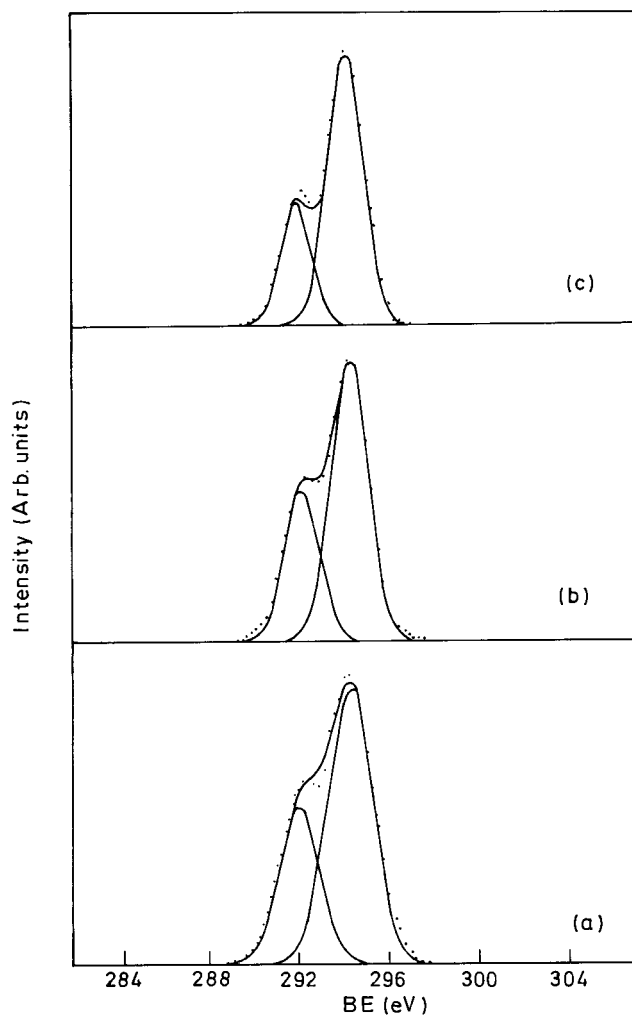


Figure 3. X-Ray photoelectron spectrum of the C 1s region of krytox 1625 fitted with two symmetric Gaussians at various electron take-off angles (dots are the original data points and smooth curves are the fits): (a) 90°, (b) 70°, and (c) 50°. The peak widths decrease with decreasing take-off angle as a result of decrease in film thickness and a consequent reduction in charging.

relative intensity of the CF peak decreases, which leads us to consider that the surface of the liquid is composed primarily of molecular ends. On such a surface there are more CF₂ and CF₃ groups than CF contributing to the C 1s intensity as the technique becomes more surface sensitive.

Figure 4 shows the C 1s spectra of krytox 16256 at electron take-off angles 90°, 70°, 50° and 30° respectively. As the surface sensitivity of the technique increases, the number of monomer units contributing to the intensity decreases. As a result, the CF₂/CF₃:CF intensity ratio increases as the observation angle decreases; this is clearly reflected in the photoelectron spectra. The actual values from the decomposed spectra are

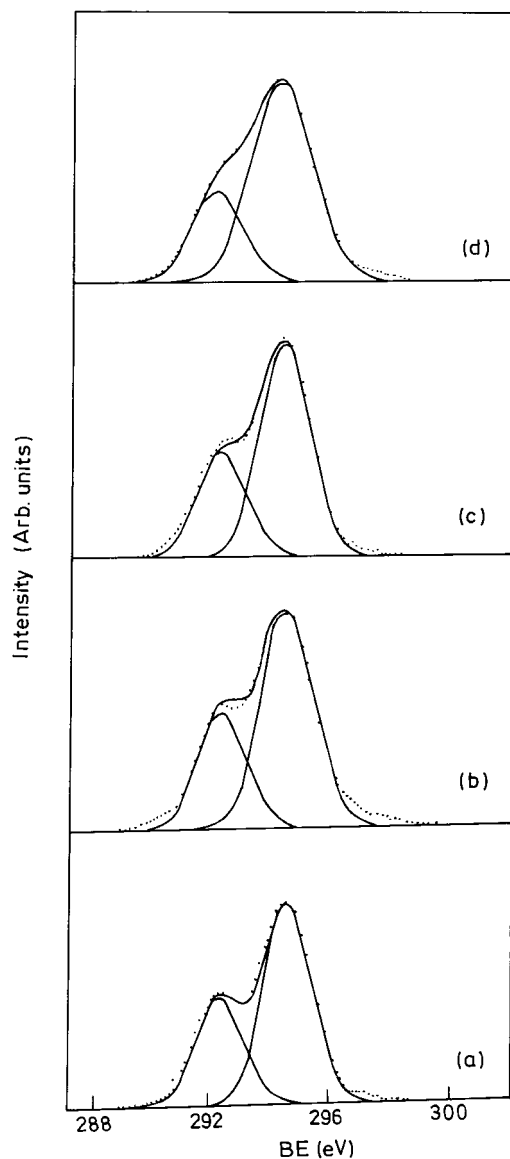


Figure 4. X-Ray photoelectron spectrum of the C 1s region of krytox 16256 fitted with two symmetric Gaussians at various electron take-off angles: (a) 90° , (b) 70° , (c) 50° , and (d) 30° .

2.00 at 90° , 2.12 at 70° , 2.25 at 50° and 2.50 at 30° . The results suggest that the molecular chain ends of the ether protrude towards the liquid surface.

In figure 5 the C 1s photoelectron spectra of krytox 16350 are shown at electron take-off angles of 80° , 60° , 40° , 20° and 10° . The spectra show exactly the same behaviour as for the other PFPE liquids. It is clear from the figure that the intensity ratio CF_2/CF_3 :CF increases with decreasing electron take-off angle. In this case, the actual intensity ratios obtained from the decomposed spectra are 1.81, 2.08, 2.12, 2.14 and 2.29 for the angles measured.

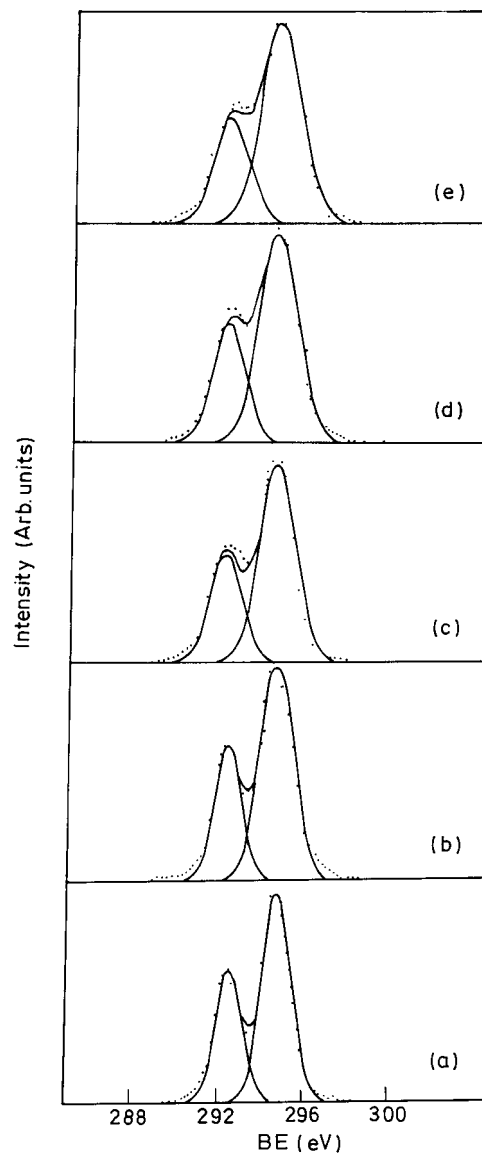


Figure 5. X-Ray photoelectron spectrum of the C 1s region of krytox 16350 fitted with two symmetric Gaussians at various electron take-off angles: (a) 80° , (b) 60° , (c) 40° , (d) 20° , and (e) 10° .

Auger spectroscopic data also suggest preferential segregation of CF_3 groups at the surface. Upon decreasing the electron take-off angle the intensity of the KVV Auger feature originating from the $K_{\text{CF}_2/\text{CF}_3}$ level increases in intensity. The Auger features are overlapping and a detailed description is impossible in the absence of adequate information on the valence electronic structure of these compounds.

3.2.3. Comparison between the three liquids

In figure 6, we show the variation in CF_2/CF_3 :CF ratio as a function of electron take-off angle for the

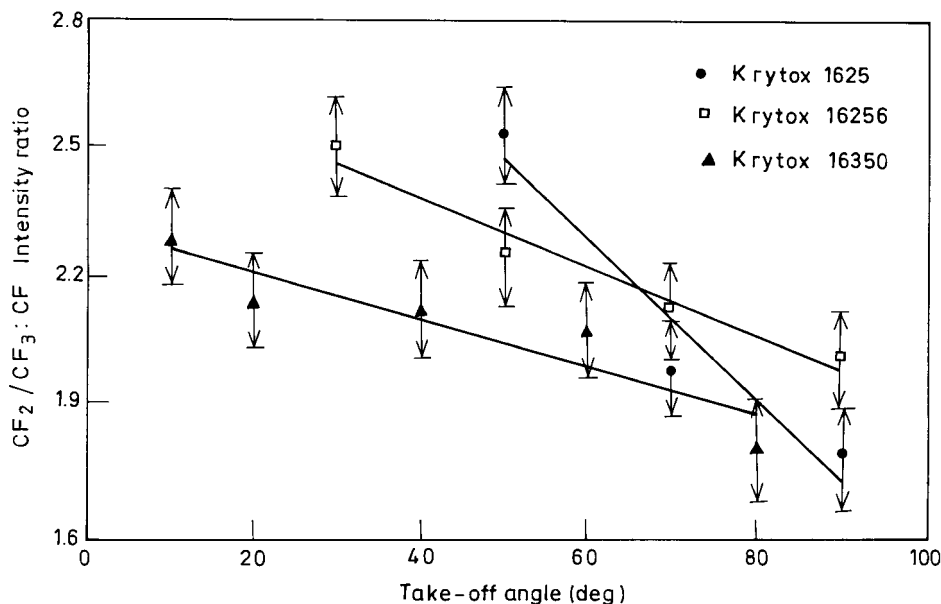


Figure 6. Plot of the variation in the CF_2/CF_3 :CF intensity ratio as a function of electron take-off angle for the three krytox liquids (lines show a least-squares fit).

three krytox liquids investigated. It is apparent from the figure that the intensity ratio varies significantly with the electron take-off angle, justifying the conclusions above. Although the variation in intensity with take-off angle need not be linear, a least-squares fit of the data has been performed. It is observed that the slope of the lines vary substantially from each other. The slopes are 0.008, 0.006 and 0.005 respectively for krytox 1625, krytox 16256 and krytox 16350 liquids. The figure shows that the relative enhancement of CF_2/CF_3 intensity per unit change in angle is larger for liquids of lower chain length. In other words, the surface segregation of CF_3 per unit enhancement in surface sensitivity is larger for liquids of lower chain length. As the polymer chain length increases, inter-chain interactions tend to increase, which makes the surface of an infinite chain polymer similar to the bulk. The results seem to suggest that, of the liquids investigated, krytox 1625 has a more rapid change in properties as one approaches the surface. In krytox 16350 this change is rather gradual, which is manifested as a decrease in the slope.

The variation in CF_2/CF_3 :CF intensity ratio with electron take-off angle for different liquids suggests that the molecular orientations in the three liquids have certain differences. A study of lower chain length liquids suggests that for $n = 27$, 65 and >70 the geometries are not substantially different, although there is some small difference in helicity. An increase in helicity would imply a greater number of CF groups per unit depth, and therefore the intensity ratio would be lower for a larger chain length. However, as figure 2 shows, the variation in monomer length beyond a certain chain length will be extremely small. Therefore, change in

the CF_2/CF_3 :CF intensity ratio due to helicity alone in the liquids investigated would be insignificant.

However, there is another reason for the observed behaviour: the variation in tilt angle of the molecular chains (with respect to the surface normal) in these liquids. The variation in CF_2/CF_3 :CF number ratio for different tilt angles is shown in figure 7. The values have been calculated for $\text{F}[\text{CF}(\text{CF}_3)\text{CF}_2\text{O}]_{20}\text{CF}_2\text{CF}_3$ taking the optimized structural parameters of $\text{F}[\text{CF}(\text{CF}_3)\text{CF}_2\text{O}]_n\text{CF}_2\text{CF}_3$. As the molecules arrange themselves at different tilt angles, for a given depth of surface investigated, the chain length probed varies. As a larger and larger chain length is accessible, the number of CF groups investigated increases. Therefore larger deviation from a near normal arrangement results in less pronounced variation in CF_2/CF_3 :CF ratio with electron take-off angle. This is indeed the case in figure 6. Since an exact measure of the mean free path is not available, absolute value of the tilt angle is not estimated. However, the above reasoning explains the experimental facts qualitatively.

The F 1s and O 1s regions were studied as a function of electron take-off angle. In all the three PFPEs, the F 1s shows a single peak at 688.6 eV and the peak shape and intensity do not show any change with electron take-off angle. As expected, the O 1s also appears as only one peak, at 536.8 eV, which also shows the same behaviour with change in take-off angle. Since all the three PFPE liquids show the same trend, only one set of F 1s (figure 8) and O 1s (figure 9) spectra of krytox 16350, at electron take-off angles of 80° , 40° , 20° and 10° , are shown. Deliberate exposure of the surfaces to molecules such as water and PCl_3 did not show any

Figure 7. Plot of the variation of the CF_2/CF_3 : CF number ratio with variation in the tilt angle. In (a) the molecule is arranged perpendicular to the surface; in (b) the molecule is arranged to lie 20° tilted from the surface normal, and in (c) the tilt angle is 40° .

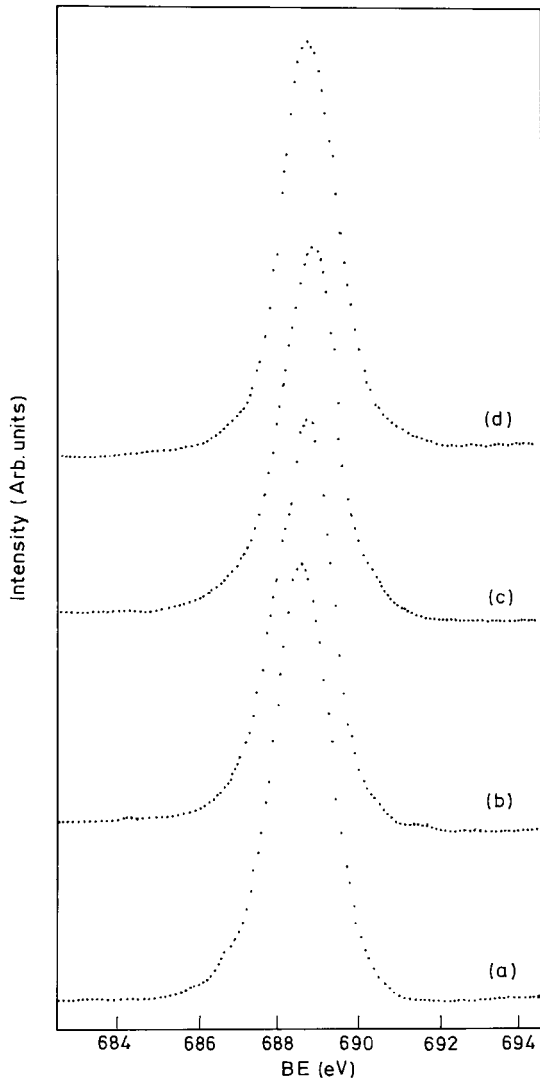
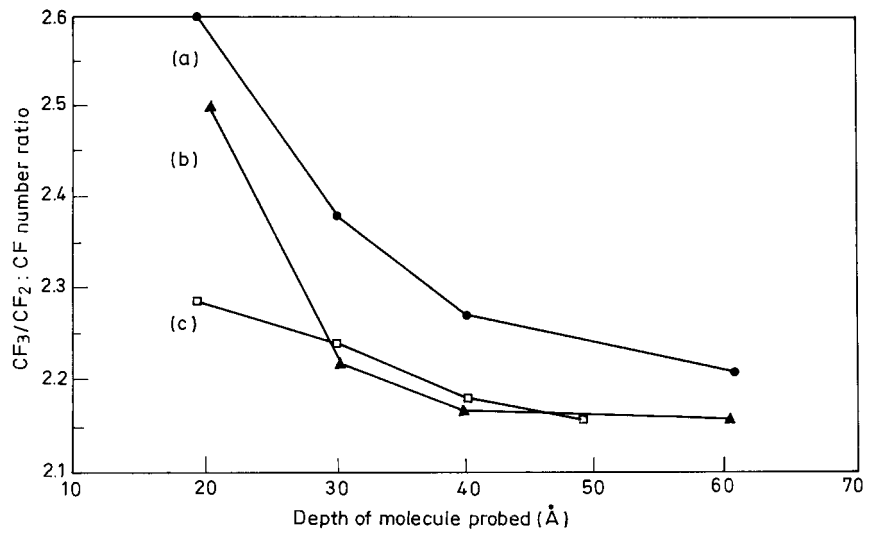


Figure 8. X-Ray photoelectron spectrum of the F 1s region of krytox 16350 at various electron take-off angles: (a) 80° , (b) 60° , (c) 29° , and (d) 10° .

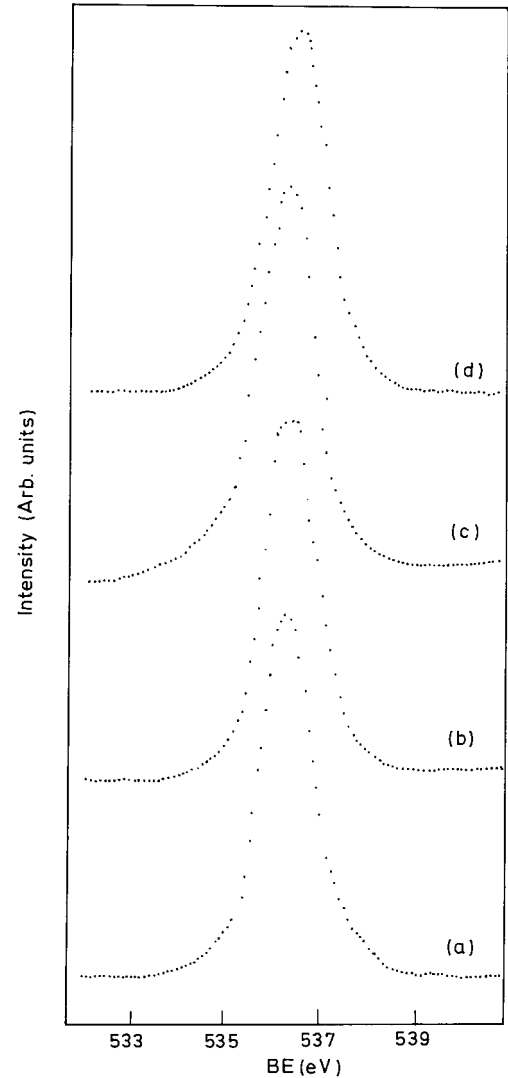


Figure 9. X-Ray photoelectron spectrum of the O 1s region of krytox 16350 at various electron take-off angles: (a) 80° , (b) 60° , (c) 20° , and (d) 10° .

adsorption, indicating that the ether oxygens are beneath the surface. The present study is in agreement with the previous ion/surface scattering [18, 19] and rare gas atom scattering [22] experiments. It can be concluded that the surfaces are composed primarily of chain ends.

4. Conclusion

In conclusion, the present study shows that a combined use of X-ray photoelectron spectroscopy and theoretical calculations can reveal details of the molecular structure of liquid surfaces. Although the requirement of an ultra high vacuum imposes certain restrictions on the suitability of this method for other systems, the technique can indeed be used for a variety of liquid surfaces. The present study performed on a series of perfluoroethers suggests that their surfaces are composed primarily of molecular terminal groups. A more rapid change in the CF₃ concentration at the surface is apparent in the lower molecular weight liquids. This is due primarily to an increasing tilt of molecules from the near normal arrangement with increase in chain length. Added to this, the increase in helicity is also an important reason. Auger electron spectroscopic measurements support the XPS data. Adsorption experiments indicate that the ether oxygen atoms are not available for any of the surface processes. The results are in agreement with atomic, molecular and ion beam scattering experiments, and theoretical calculations. A comprehensive understanding of the photoelectron spectra does require theoretical simulations of the molecular structure of the liquid. Conversely, modelling of the liquid surface on the basis of experimental XPS intensities is also possible.

T.P. thanks the Department of Science and Technology, New Delhi, Rajiv Gandhi Foundation and the Jawaharlal Nehru Centre for Advanced Scientific Research for financial support. K.S. thanks the CSIR, Government of India for a graduate student fellowship.

References

- [1] SAECKER, M. E., and NATHANSON, G. M., 1993, *J. chem. Phys.*, **99**, 7056.
- [2] HARRIS, J. G., 1992, *J. phys. Chem.*, **96**, 5077.
- [3] LEE, D. J., TELO DE GAMA, M. M., and GUBBINS, K. E., 1984, *Molec. Phys.*, **53**, 1113.
- [4] SALMONS, E., and MARESCHAL, M., 1991, *J. Phys.: condens. Matter*, **3**, 3545.
- [5] CHAPELA, G. A., SAVILLE, G., THOMPSON, S. M., and ROWLINSON, J. S., 1977, *J. chem. Soc. Faraday Trans. II*, **73**, 1133.
- [6] TOWNSEND, R. M., GRYKO, J., and RICE, S. A., 1985, *J. chem. Phys.*, **83**, 4391.
- [7] BENJAMIN, I., and PUHORILLE, A., 1993, *J. chem. Phys.*, **98**, 236.
- [8] MATSUMOTO, M., and KATAOKA, Y., 1989, *J. chem. Phys.*, **90**, 2398.
- [9] TOWNSEND, R. M., and RICE, S. A., 1991, *J. chem. Phys.*, **94**, 2207.
- [10] WILSON, M. A., PUHORILLE, A., and PRATT, L. A., 1988, *J. chem. Phys.*, **88**, 3281.
- [11] LANGEVIN, D. L., 1992, *Light Scattering by Liquid Surfaces* (New York: Marcel Dekker).
- [12] PERSHAN, P. S., 1990, *Faraday Discuss. chem. Soc.*, **89**, 231.
- [13] LEE, E. M., and THOMAS, R. K., 1989, *Physica B*, **156/157**, 525.
- [14] See for a review, KASI, S. R., KANG, H., SASS, C. S., and RABALAIS, J. W., 1989, *Surface Sci. Rep.*, **10**, 1.
- [15] PRADEEP, T., AST, T., COOKS, R. G., and FENG, B., 1994, *J. phys. Chem.*, **98**, 9301.
- [16] PRADEEP, T., RIEDERER JR., D. E., HOKE II, S. H., AST, T., COOKS, R. G., and LINFORD, M. R., 1994, *J. Amer. chem. Soc.*, **116**, 8658.
- [17] SMITH, R., HARRISON JR., D. E., and GARRISON, B. J., 1989, *Secondary Ion Mass Spectrometry SIMS VII* (New York: Wiley).
- [18] PRADEEP, T., MILLER, S. A., and COOKS, R. G., 1993, *J. Amer. Soc. Mass Spectrom.*, **4**, 769.
- [19] PRADEEP, T., MILLER, S. A., ROHRS, H. W., FENG, B., and COOKS, R. G., 1995, *Mater. Res. Soc. Symp. Proc.*, **380**, 93.
- [20] SAECKER, M. E., and NATHANSON, G. M., 1994, *J. chem. Phys.*, **100**, 3999.
- [21] KING, M. E., NATHANSON, G. M., HANNING-LEE, M. A., and MINTON, T. K., 1993, *Phys. Rev. Lett.*, **70**, 1026.
- [22] SAECKER, M. E., GOVONI, S. T., KOWALSKI, D. V., KING, M. E., and NATHANSON, G. M., 1991, *Science*, **252**, 1421.
- [23] ROJSTACZER, S., REE, M., YOON, D. Y., and VOLKSEN, W., 1992, *J. Polym. Sci. B*, **30**, 133.
- [24] TONEY, M. F., and BRENNAN, S., 1990, *J. chem. Phys.*, **92**, 3781.
- [25] TIDSWELL, I. M., OCKO, B. M., PERSHAN, P. S., WASSERMAN, S. R., WHITESIDES, G. M., and AXE, J. D., 1990, *Phys. Rev. B*, **41**, 1111.
- [26] KELLER, W., MORGNER, H., and MULLER, W. A., 1986, *Molec. Phys.*, **57**, 623.
- [27] GOH, G. C., HICKS, J. M., KEMNITZ, K., PINTO, G. M., BHATTACHARYYA, K., EISENTHAL, K. B., and HEINZ, T. F., 1988, *J. phys. Chem.*, **92**, 5074.
- [28] SUPERFINE, R., HUANG, J. Y., and SHEN, Y. R., 1991, *Phys. Rev. Lett.*, **66**, 1066.
- [29] MATSUMOTO, M., and KATAOKA, Y., 1988, *J. chem. Phys.*, **88**, 3233.
- [30] GOMER, R., and TRYSON, G., 1977, *J. chem. Phys.*, **66**, 4413; MADDEN, W. G., GOMER, R., and MANDELL, M. J., 1977, *J. phys. Chem.*, **81**, 2652.
- [31] CLARK, D. T., and THOMAS, H. R., 1977, *J. Polymer Sci.*, **15**, 2843; SASTRY, M., GANGULY, P., BADRINARAYANAN, S., MANDALE, A. B., SAINKAR, S. R., PARANJAPE, D. V., PATIL, K. R., and CHAUDHARY, S. K., 1991, *J. chem. Phys.*, **95**, 8631; BRUNDLE, C. R., HOPSTER, H., and SWALEN, J. D., 1979, *J. chem. Phys.*, **70**, 5190.
- [32] RAMASAMY, S., and PRADEEP, T., 1995, *J. chem. Phys.*, **103**, 485.
- [33] PRADEEP, T., 1995, *Chem. Phys. Lett.*, **243**, 125.
- [34] BINDU, V., and PRADEEP, T., 1997, *J. chem. Phys.*, **106**, 1231.

- [35] Du Pont, Wilmington, DE, *Krytox series of lubricants*.
- [36] FRISCH, M. J., TRUCKS, G. W., SCHLEGEL, H. B., GILL, P. M. W., JOHNSON, B. G., ROBB, M. A., CHEESEMAN, J. R., KEITH, T. A., PETERSSON, G. A., MONTGOMERY, J. A., RAGHAVACHARI, K., AL-LAHAM, M. A., ZAKRZEWSKI, V. G., ORTIZ, J. V., FORESMAN, J. B., CIOSLOWSKI, J., STEFANOV, B. B., NANAYAKKARA, A., CHALLACOMBE, M., PENG, C. Y., AYALA, P. Y., CHEN, W., WONG, M. W., ANDRES, J. L., REPLOGLE, E. S., GOMPERTS, R., MARTIN, R.L., FOX, D. J., BINKLEY, J. S., DEFREES, D. J., BAKER, J., STEWART, J. P., HEAD-GORDON, M., GONZALEZ, C., and POPLE, J. A., 1995, *Gaussian 94* (Pittsburgh, PA: Gaussian, Inc.).
- [37] POPLE, J. A., and SEGAL, G. A., 1966, *J. chem. Phys.*, **44**, 3289.
- [38] POPLE, J. A., and BEVERIDGE, D. L., 1970, *Approximate Molecular Orbital Theory* (New York: McGraw-Hill).
- [39] MURREL, J. N., and HARGET, A. J., 1972, *Semi-Empirical Self-Consistent-Field Molecular Orbital Theory of Molecules* (New York: Wiley).
- [40] MADISON, N. L., and KOO, G. P., 1972, *Fluoropolymers* (New York: Wiley).